

**Empirical mode decomposition and synchrogram approach to cardiorespiratory synchronization**

Ming-Chya Wu\* and Chin-Kun Hu†

*Institute of Physics, Academia Sinica, Nankang, Taipei 11529, Taiwan*

(Received 22 July 2005; revised manuscript received 30 March 2006; published 24 May 2006)

We use the empirical mode decomposition method to decompose experimental respiratory signals into a set of intrinsic mode functions (IMFs), and consider one of these IMFs as a respiratory rhythm. We then use the Hilbert spectral analysis to calculate the instantaneous phase of the IMF. Heartbeat data are finally incorporated to construct the cardiorespiratory synchrogram, which is a visual tool for inspecting synchronization. We perform analysis on 20 data sets collected by the Harvard medical school from ten young (21–34 years old) and ten elderly (68–81 years old) rigorously screened healthy subjects. Our results support the existence of cardiorespiratory synchronization. We also investigate the origin of the cardiorespiratory synchronization by addressing the problem of correlations between regularities of respiratory and cardiac signals. Our analysis shows that regularity of respiratory signals plays a dominant role in the cardiorespiratory synchronization.

DOI: [10.1103/PhysRevE.73.051917](https://doi.org/10.1103/PhysRevE.73.051917)

PACS number(s): 87.19.Hh, 87.17.Aa, 05.45.–a

**I. INTRODUCTION**

The study of oscillations and couplings in physiological systems has gained increasing attention in recent decades [1–19]. On one hand, physiological systems can serve as a playground for the study of analysis techniques of nonlinear dynamics. On the other hand, the application of the existing concepts and knowledge from other fields to provide insights for solving problems in medical science has been an important and promising topic. Among these, human cardiovascular and respiratory systems have been widely studied. It has been found that these two systems do not act independently; instead, they are coupled by several mechanisms. The nature of the couplings between them has been extensively studied from measured data in recent years [18–25], and is known to be both neurological [1] and mechanical [2], and is also known to be nonlinear. The interactions between them result in the well-known modulation of heart rates known as respiratory sinus arrhythmia (RSA). Moreover, recent studies suggest that besides modulations, there is also synchronization between these two systems.

Almasi and Schmitt reported that there are voluntary synchronization between subjects' breathing and cardiac cycle [3]. They found that subjects, signaled by a tone derived from the electrocardiograms, inspired for a fixed number of heart beats followed by expiration for a fixed number of heart beats [3]. The typical pattern is two beats for inspiration and three beats for expiration; in general such pattern depends on age, tidal volume, and body position. More recently, Schäfer *et al.* [5,6] and Rosenblum *et al.* [7] applied the concept of phase synchronization of chaotic oscillators [15] to develop a technique to analyze irregular nonstationary bivariate data from cardiovascular and respiratory systems, and used the cardiorespiratory synchrogram (CRS) to detect different synchronous states and transitions between them. They found a sufficiently long period of hidden syn-

chronization and concluded that the cardiorespiratory synchronization and RSA are two competing factors in cardiorespiratory interactions. Later, Tolddo *et al.* [8] developed an algorithm to detect epochs of synchronization automatically and objectively. They further found that synchronization was less abundant in normal subjects than in transplant patients, which indicated that the physiological condition of the latter promotes cardiorespiratory synchronization.

Up to now, cardiorespiratory synchronization has been reported in young healthy athletes [5,6], healthy adults [9–11], heart transplant patients [9], infants [12], and anesthetized rats [13]. It follows that most of the studies support the existence of cardiorespiratory synchronization. However, most of the studies focused on phenomenological interpretations, and usually hoped to answer the effects of age, body position, or respiratory tidal volume on the beat-to-beat heart rate change, and of the breathing rate on heart rate variability. In addition, in recent studies the nature of coupling has been extensively investigated from measured data by synchronization theory [18,19], the information-theoretic approach [20,21], time-phase bispectral analysis [22], the nonlinear state space projection technique [23], and time series analysis based on the paradigm of deterministic chaos [24,25]. Because of the limitation of experiments, a general understanding of the mechanisms of cardiorespiratory synchronization is still lacking. To address this issue, Kotani *et al.* [14] developed a physiological model to study the phenomena from another aspect. Their model showed that both the influence of respiration on heartbeat and the influence of heartbeat on respiration are important for cardiorespiratory synchronization.

Since the studies mentioned above are based on measured data, the data processing method plays a crucial role in the obtained results. It is reasonable to assume that respiratory signals have noisy, linear, nonlinear, and nonstationary components. An essential task for studies will be to process such signals and pick up essential component(s) from experimental respiratory signals. Except for the Fourier spectral analysis that has been widely used, to date there have been several approaches to preprocess real data for this purpose. For example, the Gabor transform [26] has been used to quantify

\*Electronic address: [mcwu@phys.sinica.edu.tw](mailto:mcwu@phys.sinica.edu.tw)†Electronic address: [huck@phys.sinica.edu.tw](mailto:huck@phys.sinica.edu.tw)

and visualize the time evolution of the traditional frequency bands defined in the analysis of electroencephalograms [27]; the wavelet transform has been used to filter signals to estimate the instantaneous phase based on time-frequency methods [28–30], and the Karhunen-Loève decomposition [31,32] has been used to decompose signals into separate modes, etc. Even though proper filters can be used to filter out noise from real data, the capabilities and effectiveness of the filtration are usually questionable. This is due to the fact that most of these approaches require that the original time series should be stationary and/or linear. However, respiratory signals are noisy, nonlinear, and nonstationary. Furthermore, there are also no strict criteria to judge what is the inherent dynamics and what is the contribution of the external factors and noise in experimental respiratory signals. Improper approaches might then lead to misleading results. In addition, there are also technical problems in the analysis of respiratory signals: insufficiently filtered signals may still have too many noises, and overfiltered signals may be so regular as to lose characteristics of respiratory rhythms.

To overcome the above difficulties, here we propose to use the empirical mode decomposition (EMD) method proposed by Huang *et al.* [33] and Hilbert spectral analysis [34] as a candidate for such studies. Unlike conventional filters, the EMD method provides an effective way to extract respiratory rhythms from experimental respiratory signals. The EMD method is designated for the analysis of nonlinear and nonstationary time series, and has been used to analyze electric intracranial signals recorded from an epileptic patient [35]. The method mainly has two advantages [33,36]. (i) By the sifting process, one can eliminate most of the riding waves and make the wave profiles more symmetric. The efficiency of EMD is that the expansion of the turbulence data set has only a finite number of terms, and the completeness and orthogonality of the decomposition have been restrictively proved. (ii) The sifting process separates the data into locally nonoverlapping time scale components, known as intrinsic mode functions (IMFs). The adaptive properties of IMFs to empirical data also make it easy to give physical significance to each mode of a complicated data set, and allow us to choose a certain IMF as a respiratory rhythm. This is the key point of our analysis. After a respiratory rhythm is selected based on physical criteria, one can further use CRS to detect synchronization.

In this paper, we also address the problem of effects of signal regularities on the synchronization, and the correlations between cardiac and respiratory signals. We further design a scheme to test the reliability of simple modeling of cardiorespiratory synchronization.

This paper is organized as follows. In Sec. II, we introduce the data processing method used in this paper, and briefly review the EMD method. In Sec. III, the EMD process is used to extract the respiratory signals and the Hilbert transform is used to calculate the instantaneous phase of the respiratory time series. The CRS is then constructed by assessing heartbeat data on the phase of the respiratory signal, and is used to visually detect the epochs of synchronization. In Sec. IV we investigate the correlation between regularity of cardiac and respiratory signals and cardiorespiratory synchronization. Finally, we discuss our results in Sec. V.

## II. DATA ACQUISITION AND PROCESSING

### A. Experimental data sets

We analyze 20 data sets, which were collected by the Harvard medical school in 1994 [37]. Ten young (21–34 years old) and ten elderly (68–81 years old) rigorously screened healthy subjects underwent 120 min of continuous supine resting while continuous electrocardiographic (ECG) and respiration signals were collected. All subjects remained in a resting state in sinus rhythm while watching the movie “Fantasia” (Disney 1940) to help maintain wakefulness. The continuous ECG and respiration data were digitized at 250 Hz (respiratory signals were later preprocessed to be at 5 Hz, i.e., five data points per second). Each heartbeat was annotated using an automated arrhythmia detection algorithm, and each beat annotation was verified by visual inspection. The records f1y01, f1y02, ..., f1y10 were obtained from the young cohort, and records f1o01, f1o02, ..., f1o10 were obtained from the elder cohort. Each group of subjects includes equal numbers of men and women.

### B. The Hilbert-Huang signal analysis method

Since the respiratory signals represent measures of the volume of expansion of the ribcage, the corresponding time series are all positive numbers and there are no zero crossings. In addition to respiratory rhythms, the empirical data also contain noises originating from measurements, external disturbances, and other factors. Hence, the experimental data of respiratory signals are complicated with many local extremes. To reduce noises of the empirical data, we apply the EMD method [33] to preprocess the data. The EMD method was developed from the assumption that any time series data consist of different simple intrinsic modes of oscillation. The essence of the method is to identify the intrinsic oscillatory modes by their characteristic time scales in the data empirically, and then decompose the data accordingly [33]. This is achieved by “sifting” data to generate IMFs. The IMFs obtained by EMD are a set of well-behaved intrinsic modes, and these functions satisfy the conditions that they are symmetric with respect to the local zero mean and have the same numbers of zero crossings and extremes. Based on this property, one can select a reasonable one from IMFs as a respiratory rhythm and simply apply the Hilbert transform on it to calculate the instantaneous phase.

The algorithm to create IMFs in EMD is rather elegant, and has two main steps.

*Step 1.* First, the local extremes in the experimental respiratory time series data  $\{x(t)\}$  are identified. Then, all the local maxima are connected by a cubic spline line  $U(t)$ , which forms the upper envelope of the time series, while the same procedure is applied for the local minima to produce the lower envelope  $L(t)$ . Both envelopes will cover all of the original time series. The mean of upper envelope and lower envelope  $m_1(t)$  given by

$$m_1(t) = \frac{U(t) + L(t)}{2} \quad (1)$$

is a running mean. Subtracting the running mean  $m_1(t)$  from the original time series  $x(t)$  we get the first component  $h_1(t)$ ,

$$x(t) - m_1(t) = h_1(t). \quad (2)$$

The resulting component  $h_1(t)$  is an IMF if it satisfies the following conditions: (i)  $h_1(t)$  is free of riding waves; (ii) it displays symmetry of the upper and lower envelopes with respect to zero; (iii) the numbers of zero crossing and extremes are the same, or only differ by 1. Besides these, an additional condition based on the intermittence (i.e., varying numbers of data points per cycle; see the explanation below) can be imposed here to sift out waveforms with a certain range of intermittence for the purpose of physical consideration. If  $h_1(t)$  is not an IMF, the sifting process has to be repeated as many times as is required to reduce the extracted signal to an IMF.

In the subsequent sifting process steps,  $h_1(t)$  is treated as the data to repeat the steps mentioned above,

$$h_1(t) - m_{11}(t) = h_{11}(t). \quad (3)$$

Again, if the function  $h_{11}(t)$  does not yet satisfy criteria (i)–(iii), the sifting process continues up to  $k$  times until some acceptable tolerance is reached:

$$h_{1(k-1)}(t) - m_{1k}(t) = h_{1k}(t). \quad (4)$$

*Step 2.* If the resulting time series is the first IMF, it is designated as  $c_1 = h_{1k}(t)$ . The first IMF is then subtracted from the original data, and the difference  $r_1$  given by

$$x(t) - c_1(t) = r_1(t) \quad (5)$$

is the first residue. The residue  $r_1(t)$  is taken as if it were the original data and we apply to it again the sifting process of step 1.

Following the above procedures of step 1 and step 2, we continue the process to find more intrinsic modes  $c_i$  until the last one. The final residue will be a constant or a monotonic function which represents the general trend of the time series. Finally, we get

$$x(t) = \sum_{i=1}^n c_i(t) + r_n(t), \quad (6)$$

$$r_{i-1}(t) - c_i(t) = r_i(t). \quad (7)$$

Figure 1 shows typical results from EMD.

Having obtained IMFs, one can select one component as the respiratory rhythm according to the criteria of intermittencies of IMFs imposed in step 1 as an additional sifting condition. Note that among these IMFs, the first IMF has the highest oscillatory frequency, and in our practical EMD process, there is a general relation of intermittence for different modes:

$$\tau_n = 2^{n-1} \tau_1, \quad (8)$$

where  $\tau_n$  denotes the intermittence of the  $n$ th mode. In other words, if  $c_1$  has intermittence ranging from  $\tau_1$  to  $2\tau_1$ , then the  $c_n$  mode has intermittence ranging from  $2^{n-1}\tau_1$  to  $2^n\tau_1$ .

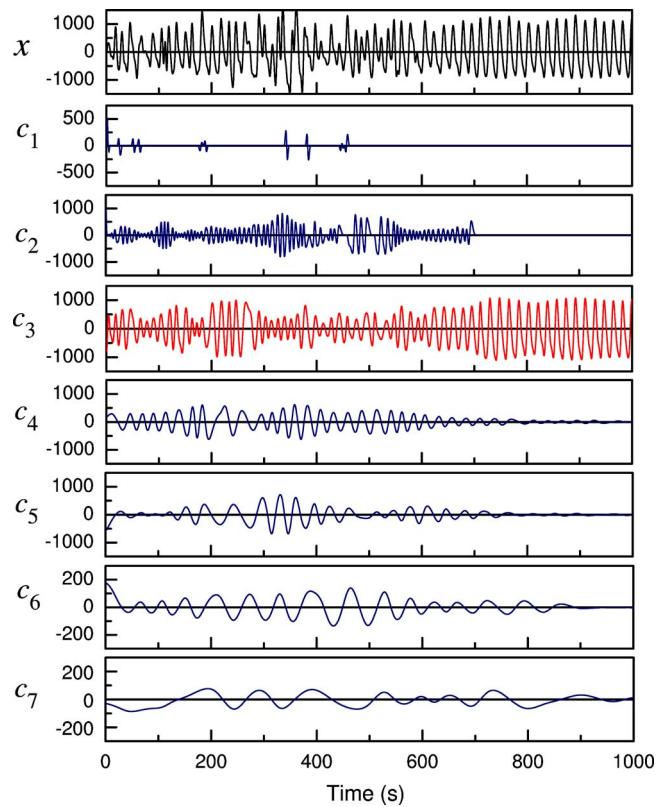


FIG. 1. (Color online) Example of EMD for a typical respiratory time series data (code flo01 in our study). The criteria for intermittence in the sifting process is 3–6 data points per cycle for  $c_1$ . Signal  $x(t)$  is decomposed into 14 components including 13 IMFs and one residue; here only the first seven components are shown.

After one of the IMFs is selected as the respiratory rhythm, one further applies the Hilbert transform to the selected IMF, say the  $r$ th component  $c_r(t)$ . The procedures of the Hilbert transform consist of calculation of the conjugate pair of  $c_r(t)$ , i.e.,

$$y_r(t) = \frac{1}{\pi} \text{P} \int_{-\infty}^{\infty} \frac{c_r(t')}{t-t'} dt', \quad (9)$$

where P indicates the Cauchy principal value. With this definition, two functions  $c_r(t)$  and  $y_r(t)$  forming a complex conjugate pair define an analytic signal  $z_r(t)$ :

$$z_r(t) = c_r(t) + iy_r(t) \equiv A_r(t)e^{i\phi_r(t)}, \quad (10)$$

with amplitude  $A_r(t)$  and the instantaneous phase  $\phi_r(t)$  defined by

$$A_r(t) = [c_r^2(t) + y_r^2(t)]^{1/2}, \quad (11)$$

$$\phi_r(t) = \arctan\left(\frac{y_r(t)}{c_r(t)}\right). \quad (12)$$

### C. Data processing

The number of breaths per minute for human beings has a rather wide range; it is about 18 cycles in one minute for

adults, and about 26 cycles in one minute for children. For different healthy states, the number of cycles may also vary case by case. To include most of these possibilities, one should take respiratory cycles ranging from 10 to 30 times per minute, and each respiratory cycle then roughly takes 2–6 s, i.e., 10–30 data points.

The procedures of data processing in this paper are as follows. (i) Apply the EMD to decompose the recorded data into several IMFs. The decomposition acquires input of the number of sifting times and criteria of intermittence as the parameters in the sifting process, and we use the time scale of a respiratory cycle as the criterion. The number of sifting times generally depends on the data quality, and it varies case by case. Since the respiratory signal was preprocessed to a sampling rate of 5 Hz, there are 10–30 data points in one cycle. Then, for example, we can use  $c_1$ : 3–6,  $c_2$ : 6–12,  $c_3$ : 12–24, etc. After the sifting processes of EMD, the original respiratory data are decomposed into  $n$  empirical modes  $c_1, c_2, \dots, c_n$ , and a residue  $r_n$ . (ii) Visually inspect the resulting IMFs decomposed by the EMD. If the amplitude of a certain mode is dominant and the wave form is well distributed, then the data are said to be well decomposed and the decomposition is successfully completed. Otherwise, the decomposition may be inappropriate, and we have to repeat step (i) with different parameters.

The physical meaning of IMFs can be understood from their intermittencies. Here we should note that the variability of respiratory signals is substantially preserved in a certain IMF by using the property of the adaptive basis instead of the *a priori* basis in other methods, such as Fourier-based analysis and wavelet methods [33]. In other words, the frequency in the EMD method is not global, but is local in time (i.e., time dependent). The range of intermittence imposed on the sifting process can be adapted according to the physiological condition revealed from empirical respiratory signals. Thus, the whole scheme is adaptive and self-consistent. Here we should emphasize that in our study, only one IMF should be taken for the respiratory rhythm and any sum of a few IMFs cannot be used. This is due to the fact that the Hilbert transform must be performed on an IMF to yield correct phases with physical significance [33]. However, a sum of two or more IMFs is never an IMF. Therefore, one should properly choose the intermittence such that the respiratory time signal can be correctly gathered into a single IMF. The resultant benefit is that those IMFs having smaller or larger intermittencies can be considered as noises involved in the experiments or signals originating from sources other than the respiratory system. The above requirement can be easily achieved by the property of the EMD method in which adaptive bases (i.e., IMFs) are generated by tuning the intermittence in the sifting procedure, and the performance of the method can be examined by comparing original data and the resultant IMFs.

For example, in Fig. 1, the empirical signal was decomposed with a criteria of the intermittence being 3–6 data points for  $c_1$ , and  $3 \times 2^{n-1} - 3 \times 2^n$  data points for  $c_n$ 's with  $n > 1$ . Comparing  $x(t)$  with the  $c_i$ 's, it is obvious that  $c_3$  preserves the main structure of the signal and is dominant in the decomposition. We thus pickup the third component  $c_3$ , corresponding to 12–24 data points per respiratory cycle,

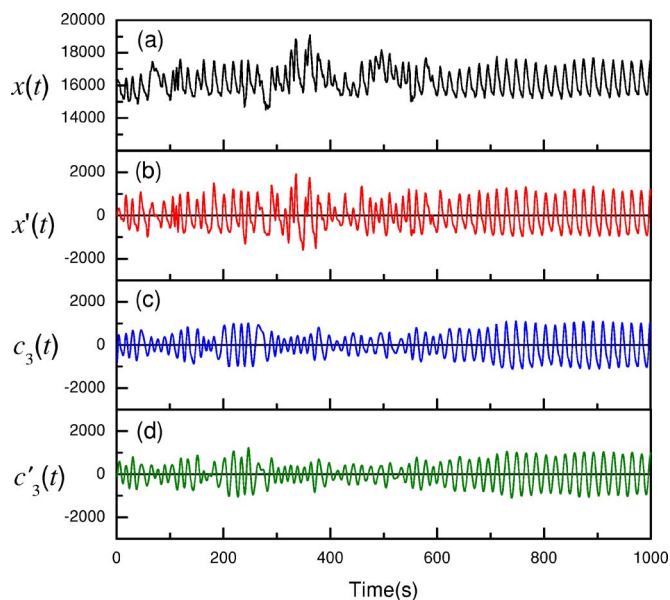


FIG. 2. (Color online) Comparison of respiratory signals for a typical subject (code f1o01) in different data processing stages: (a) original experimental time series  $x(t)$ , (b) after performing low-pass filtering,  $x'(t)$ , (c) the third IMF  $c_3(t)$  in Fig. 1, after performing EMD on  $x'(t)$ , and (d) the postprocessed signal  $c_3'(t)$  after performing the Fourier spectrum analysis.

as the respiratory rhythm. Note that for strongly noisy data, this may not be the case, and the decomposition becomes difficult. Then, we can optionally filter empirical data by proper filters, and then apply the EMD. Figure 2 compares respiratory signal in various stages. In Fig. 2(a), a typical respiratory time series  $x(t)$  is shown. The preprocessed signal  $x'(t)$  by a proper Fourier band filter is shown in Fig. 2(b), in which only fast oscillatory noises are filtered out, and the main structures of the signal are preserved. Figure 2(c) shows the IMF  $c_3(t)$  obtained by performing EMD on  $x'(t)$ . The process is similar to that used to obtain  $c_3(t)$  in Fig. 1. Obviously, the IMF  $c_3(t)$  of Fig. 2(c) still preserves characteristic structure of  $x(t)$  shown in Fig. 2(a).

Here we note that the sifting processes in the EMD separate the data into locally nonoverlapping time scale components. Sometimes this leads to the situation that there is no signal in some time period, due to higher oscillatory behaviors or noises in that period. If this occurs, one can optionally use the Fourier spectrum analysis to recover the signal in that period. For example, we can use the discrete Fourier transform technique, and take

$$c_3'(t) = \frac{4}{N} \sum_{f=f_L}^{f_H} \left( \sum_{n=0}^N c_3(n) e^{i2\pi n f/N} \right) e^{-i2\pi f t/N}, \quad (13)$$

where  $N$  is the total number of data points of the respiratory time series,  $f_H$  is the high-frequency limit, and  $f_L$  is the low-frequency limit. The values of  $f_H$  and  $f_L$  can be chosen as  $6/\Delta t$  and  $2/\Delta t$ , respectively. However, we should inspect the resulting signal visually to confirm whether the filtering is applicable. Figure 2(d) shows the data postprocessing func-

tion  $c_3'(t)$ , which is obtained by performing the Fourier spectrum analysis on  $c_3(t)$  in Fig. 2(c). It is preferable to require that data postprocessing preserve the characteristic structures of  $c_3(t)$ , and has effects only on the time period of the blank signal. It follows that this postprocessing step is usually unnecessary.

After the above data processing scheme, the respiratory rhythms are clean enough for further analysis. We can then proceed in the next step to construct the CRS.

### III. THE CARDIORESPIRATORY SYNCHROGRAM

Cardiorespiratory synchronization is considered as a process of adjustment of rhythms due to physiological interactions between subsystems. These interactions can lead to a perfect locking of their phases, whereas their amplitudes remain chaotic and noncorrelated [4]. Let us now denote the phase of the respiratory signal calculated by Eq. (12) as  $\phi_r$  and the heartbeat as  $\phi_c$ . If the two phases are coupled in a fashion that the cardiovascular system completes  $m$  heartbeats in  $n$  respiratory cycles, then a roughly fixed relation can be proposed. In general, there will be the phase locking condition [4–6]

$$|n\phi_r - m\phi_c| = \text{const}, \quad (14)$$

with  $m, n$  integer, or a weaker type of synchronization named frequency locking [4,6],

$$|n\phi_r - m\phi_c| < \text{const}. \quad (15)$$

More precisely, frequency locking should be regarded as modulation but not synchronization [6]. Note that Eq. (15) is often considered as a condition for phase locking because the phase difference in noisy systems fluctuates and cannot be a constant as shown in Eq. (14), and a loose condition (i.e.,  $|n\phi_r - m\phi_c| \leq \text{const}$ ) is used for the phase locking. In this paper we use stricter conditions to distinguish the two types of synchronization.

According to Eq. (14), for the case that the ECG completes  $m$  cycles while the respiration completes  $n$  cycles, it is said to be a synchronization of  $m$  cardiac cycles with  $n$  respiratory cycles. Using the heartbeat event time  $t_k$  as the time frame in which the length of time intervals are not fixed, but vary with the time, then Eq. (14) implies the relation

$$\phi_r(t_{k+m}) - \phi_r(t_k) = 2\pi n. \quad (16)$$

Furthermore, by defining

$$\Psi_m(t_k) = \frac{1}{2\pi} [\phi_r(t_k) \bmod 2\pi n] \quad (17)$$

and plotting  $\Psi_m(t_k)$  versus  $t_k$ , synchronization will result in  $n$  horizontal lines in the case of  $n:m$  synchronization. By choosing  $n$  adequately, a CRS which is a visual tool can be developed for detecting the synchronization between heartbeat and respiration [5,6].

An example of 3:1 synchronization with  $n=6$  and  $m=2$  is shown in Fig. 3(a), where phase locking appear in several epochs, e.g., at 2800–3600 s, and there is also frequency

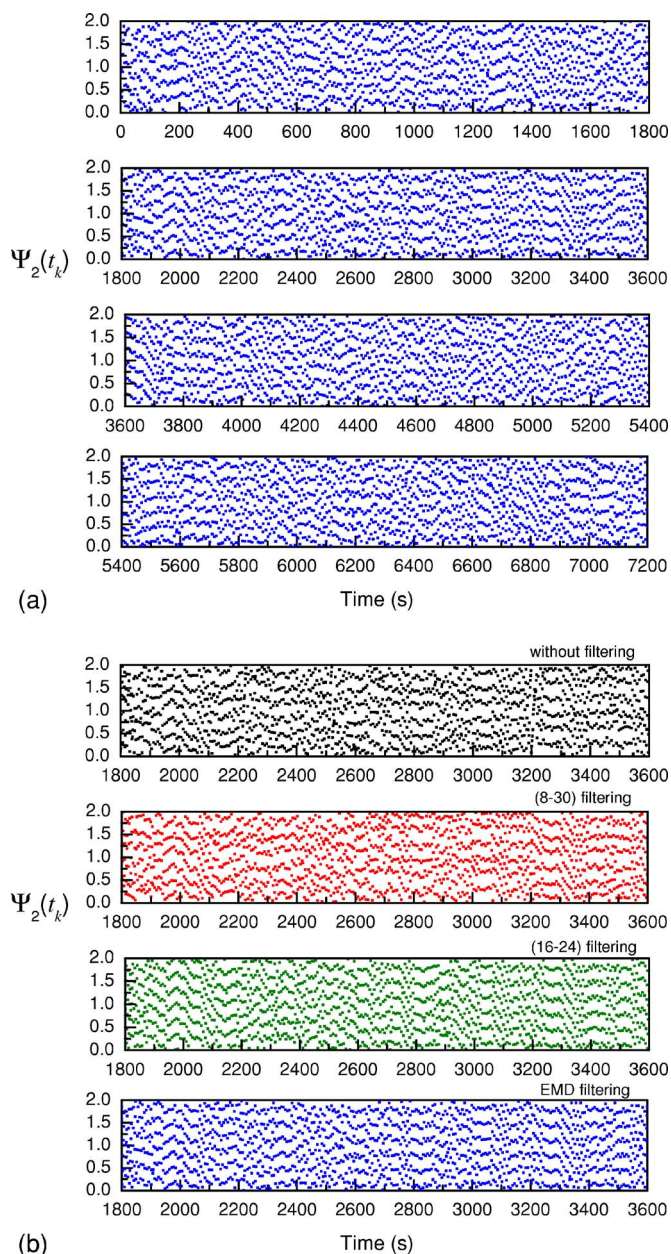


FIG. 3. (Color online) Cardiorespiratory synchronogram for a typical subject (code fl006). (a) Empirical data are preprocessed by the EMD method. There is about 800 s synchronization at 2800–3600 s, and several spells of 50–300 s at other time intervals. (b) Comparison of the results without filtering (top), preprocessed by the standard filters with windows of 8–30 and 16–24 cycles per minute (second and third), and the EMD method (bottom).

locking, e.g., at 400 s, near which there are  $n$  parallel lines with the same positive slope. For the purpose of comparison, we also show the results of the same subject at 1800–3600 s, but with respiratory signals without filtering, preprocessed by the standard filters and the EMD method, in Fig. 3(b). The windows of the standard filters are 8–30 and 16–24 cycles per min. In general, some noise dressed signals can still show synchronization in some epochs but the Hilbert spectral analysis failed at some time intervals (e.g.,

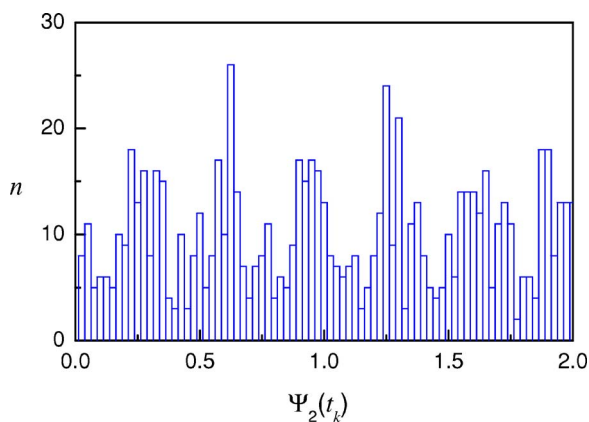


FIG. 4. (Color online) Histogram of phase for the phase locking period from 2800 to 3600 s for a typical subject (code f1o06) shown in Fig. 3(a).

around 3400–3600 s of the case without filtering), and over-filtered signals reveal too strong synchronization (filter with window of 16–24). In other words, the global frequency used in standard filters may dissolve local structures of the empirical data. This does not happen in the EMD filtering. More specifically, the advantage of the EMD method is that it is a nonlinear time-scale-based filter and a particular IMF can be properly designed to catch the variability of the respiratory signal as completely as possible.

Figure 4 shows the histogram of phases for the phase locking period from 2800 to 3600 s in Fig. 4(a). Significant higher distributions can be found at

$\Psi_2 \approx 0.25, 0.6, 0.9, 1.25, 1.6, 1.9$  in units of  $2\pi$ , indicating that heartbeat events occur roughly at these respiratory phases during this period.

Following the above procedures, we analyze the data of 20 subjects, and the results are summarized in Table I. The results are ordered by the strength of the cardiorespiratory synchronization, which is the total time length of synchronization. From our results, we do not find specific relations between the occurrence of synchronization and sex of the subjects as in Refs. [5,6] Here we note that if we used the intermittency as the bandwidth of a generic Fourier-based filter to filter the same empirical data, we will have different results depending on the strength of synchronization. For example, for the f1o06 subject, the intermittency of the third IMF is 12–24. Using 12–24 as the bandwidth of the generic Fourier-based filter, we have similar epochs of synchronization. However, for the f1y02 subject with intermittency of the second IMF 16–32 selected to optimize the decomposition, we have more epochs of 3:1 synchronization lasting 50 s and fewer 7:2 synchronization periods lasting 50 and 80 s when the bandwidth of 16–32 is used. For the f1o05 subject in which the second IMF with intermittency 10–20 is selected, epochs of 5:2 synchronization lasting 50 s are found when the same bandwidth 10–20 is used. In comparison with the results presented in Table I, the Fourier-based filter with a bandwidth of the same intermittency appears to smooth the data to have a more regular wave form, and in turn may lead to a conclusion of stronger synchronization than is the case. For a time series with variable intermittencies, the smoothing of data may introduce additional modes which do not exist in some segments

TABLE I. Summary of our results. 20 subjects are ordered by the strength (total time length) of the cardiorespiratory synchronization.  $\sigma$  is a measure of the variance for cardiac signals.

Code	Sex	Age	Synchronization	$\sigma$
f1o06	F	74	3:1 (800,300,250,150,100,50 s)	0.0009
f1y05	M	23	3:1 (350,300,200,100 s)	0.0105
f1o03	M	73	3:1 (200,50,30 s)	0.0026
f1y10	F	21	7:2 (200,50 s), 4:1 (50 s)	0.0079
f1o07	M	68	7:2 (120,100,80 s)	0.0048
f1o02	F	73	3:1 (100 s, several spells of 50 s)	0.0019
f1y01	F	23	7:2 (several spells of 30 s)	0.0087
f1y04	M	31	5:2 (80,50,30 s)	0.0156
f1o08	F	73	3:1 (50,30 s)	0.0021
f1y06	M	30	4:1 (50,30 s)	0.0104
f1o01	F	77	7:2 (several spells of 50 s)	0.0023
f1y02	F	28	3:1 (50 s)	0.0103
f1y08	F	30	3:1 (50 s)	0.0087
f1o10	F	71	3:1 (30 s)	0.0033
f1o05	M	76	No synchronization detectable	0.0019
f1y07	M	21	No synchronization detectable	0.0404
f1y09	F	32	No synchronization detectable	0.0077
f1y03	M	34	No synchronization detectable	0.0043
f1o09	M	71	No synchronization detectable	0.0164
f1o04	M	81	No synchronization detectable	0.0076

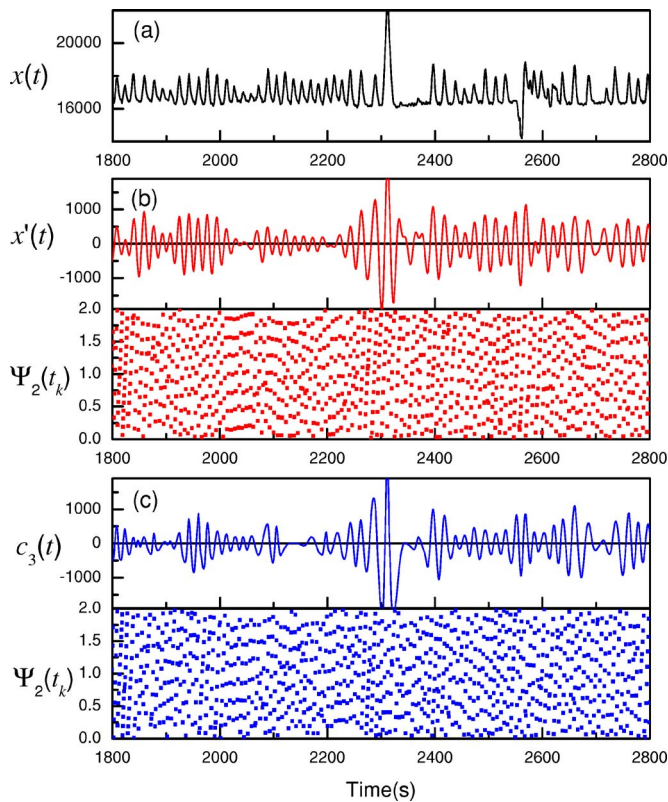


FIG. 5. (Color online) Comparison of the data processing for a typical subject (code fly02). (a) The empirical time series, (b) the time series filtered by a Fourier-based filter with bandwidth 16–32 and the corresponding synchrogram, and (c) the time series of the third IMF decomposed by the EMD method with intermittency 16–32 and the corresponding synchrogram.

of the primary data and thus leads to misleading results. For example, in Fig. 5, comparisons for the results of the fly02 subject obtained by using the Fourier-based filter and the EMD approach are shown. The original time series  $x(t)$  is dressed with noise such that the signal almost disappears at  $t=2320$ – $2380$  s. The Fourier-based filter introduces a new wave form at this epoch, but the new wave form cannot be processed directly by the Hilbert transform. This is not the case for the EMD method. Furthermore, at  $t=2000$ – $2100$  s, the Fourier-based filter does not preserve the structure of the original time series and leads to a conclusion of phase locking at this epoch. Therefore, from the aspect of data processing that keeps the reality of empirical data, the EMD approach is better than Fourier-based filtering.

#### IV. CORRELATION AND REGULARITY

In this section, we discuss the correlations between cardiac and respiratory signals and their regularities; we also test the effects of regularity on the occurrence of synchronization.

As mentioned above, the data processing method plays a crucial role in the analysis of real data. We have observed that overfiltered respiratory signals may lose detailed struc-

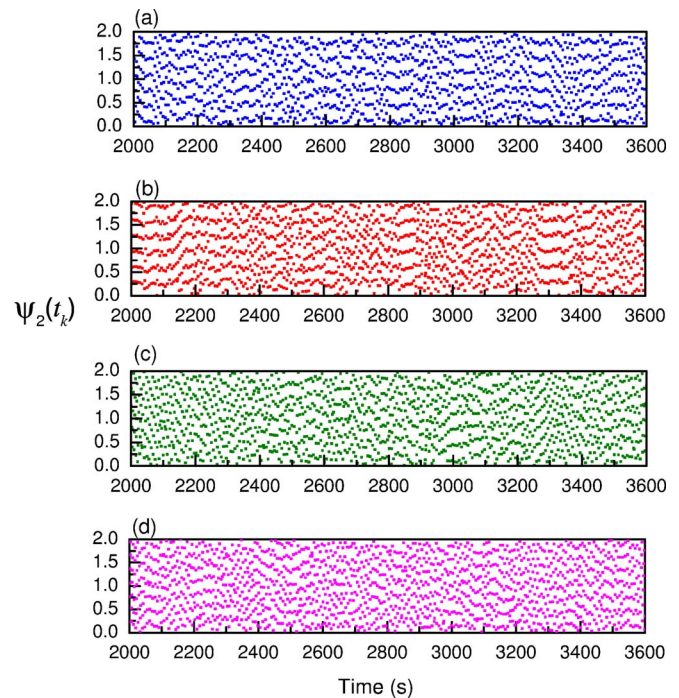


FIG. 6. (Color online) Cardiorespiratory synchrogram for data sets (a) (f1o06.res, f1o06.hrt), (b) (f1y05.res, f1y05.hrt), (c) (f1o06.res, f1y05.hrt), (d) (f1y05.res, f1o06.hrt), at period 2000–3600 s.

tures and become too regular. It follows that the final conclusions may be method dependent. One might then ask how the results depend on the data processing methods; especially, how the quality of signals affects the conclusion. This problem arises when one addresses the issue of existence or strength of the cardiorespiratory synchronization, and the answers may also be helpful for understanding or clarifying the mechanisms of the synchronization.

In general, the existence of cardiorespiratory synchronization is confirmed simply when it is proved to appear in enough subjects analyzed by various approaches. The existing studies on this topic have positive answers on its existence [5,6,9–13]. Nevertheless, the strength of synchronization for these subjects may depend on the methods one used, and need further investigation. For this purpose, we first consider two data sets (f1o06.res, f1o06.hrt) and (f1y05.res, f1y05.hrt). Here we have used the notation “code.signal” to indicate one code and a corresponding signal, and .res indicates respiratory signal and .hrt indicates heart beat signal. Both of these two data sets, codes f1o06 and f1y05, have been analyzed to show 3:1 synchronization in some periods. The synchronization exhibited by these two data sets in an interval from 2000 to 3600 s is shown, respectively, in Figs. 6(a) and 6(b). There are short spells of phase locking and frequency locking appearing in these periods. We now interchange the respiratory and cardiac time series of these sets to be (f1o06.res, f1y05.hrt) and (f1y05.res, f1o06.hrt), and then construct their synchrograms. Note that the two data sets are from real time series. The results are respectively shown in Figs. 6(c) and 6(d). There is still phase locking appearing in shorter spells for the “mixed” states, such as at 3000 s of Fig.

6(c) and at 2000 s of Fig. 6(d). This implies the synchronization (phase locking) and modulation (frequency locking) should be detectable provided that there are characteristic features coupled between respiratory and cardiac signals. Therefore, emergence of short spells of synchronization does not necessarily imply true coupling between cardiovascular and respiratory systems. If cardiorespiratory synchronization exists in a subject, the cardiovascular and respiratory systems must correlate with the same intermittence variation scheme such that synchronization can appear again and again in some time intervals. Therefore, the phase locking in the synchrogram of Fig. 3(a), where synchronization disappears and recovers repeatedly at 1800–3600 s due to the variation of intermittence of respiratory time series, indicates true cardiorespiratory synchronization.

Next, we study the dependence of the results on the regularity of signals. The regularity of a cardiac signal can be measured by the variance  $\sigma$  defined as

$$\sigma = \langle (\Delta t_n - \mu)^2 \rangle, \quad (18)$$

where  $\Delta t_n$  is the time interval between the  $n$ th heartbeat and  $(n-1)$ th heartbeat, and  $\mu$  is an average of the time intervals  $\Delta t_n$  in the period of measurement. Accordingly, a smaller value of  $\sigma$  corresponds to higher regularity. The measured values of  $\sigma$  for 20 subjects are listed in Table I, which shows that the cardiac signals are quite regular and the  $\sigma$  value is not necessarily related to the strength of synchronization. In contrast to cardiac signals, real respiratory signals are essentially irregular. Therefore, we will not measure regularity of respiratory cycles directly; instead we compare synchronization in CRS for various sets of cardiac and respiratory time series.

We then introduce an artificial respiratory signal by using a generic cosine wave  $s(S_0, T, t)$ , say,

$$s(S_0, T, t) = S_0 \cos\left(\frac{2\pi t}{T}\right), \quad (19)$$

where  $S_0$  is the amplitude, and  $T$  is the period (or somewhat similar with the intermittence in EMD). The frequency of this wave is fixed and the phase varies regularly. We then construct the synchrogram for  $[s(S_0, T, t), f1o06.hrt]$ . The results are shown in Fig. 7, in which different periods  $T=15, 16, 17, 17.6, 18$  have been used. According to Fig. 7, the cardiac signals for this subject are rather regular, and a fixed heartbeat frequency can last a relatively long time, even if it changes finally. When  $T$  is a multiple of 3, such as  $T=15$  and 18, there are synchronization spells observed at the period from 100 to 220 s, and phase locking at the other epochs. For  $T=17.6$ , phase locking can be observed at most epochs of the period. Here we should note that, in comparing Figs. 3(a) and 7, a short spell from 100 to 220 s appears as phase locking corresponds to respiratory intermittence  $T=18$ . However, a short spell from 1220 to 1350 s corresponds to respiratory intermittence roughly about  $T=17.6$ . Even though the intermittence varies, the synchronization persists. This indicates the existence of correlations.

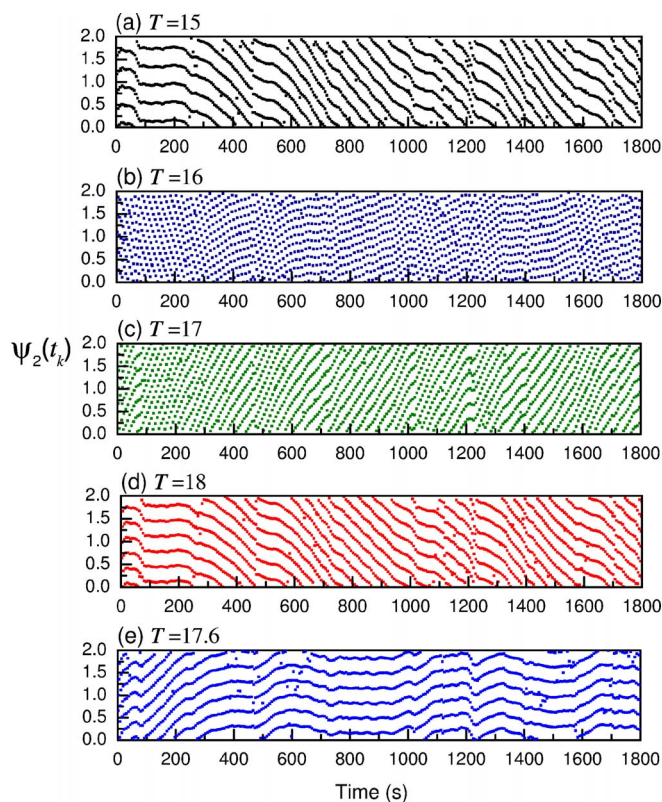


FIG. 7. (Color online) Cardiorespiratory synchrogram for data sets  $[s(S_0=1000, T, t), f1o06.hrt]$  with  $T=(a) 15, (b) 16, (c) 17, (d) 18,$  and  $(e) 17.6$ .

Comparing the patterns of the periods where synchronization occurs in Fig. 7 and the corresponding periods in Fig. 6, we find that cardiac signals are regular enough that synchronization occurs in the framework of regular time series, and respiratory cycles are not regular so that there is weaker or even no synchronization in the corresponding periods.

To have more results for comparison, we examine another subject having data set (f1o09.res, f1o09.hrt), which has no synchronization at all in the preceding analysis. The synchrogram for data set (f1o09.res, f1o09.hrt) is shown in Fig. 8(a), and data sets  $[s(S_0, T, t), f1o09.hrt]$  with  $T=15, 16, 17, 18$  are respectively shown in Figs. 8(b)–8(e). We find that there are short spells where phase locking or frequency locking appear, and the length of the spells depends on the period  $T$ . Therefore, more regular respiratory signals have better manifestation of synchronization.

From the above observations, we find the following.

(1) In most cases, cardiac oscillations are more regular than respiratory oscillations and the respiratory signal could be the key factor to determine the strength of the cardiorespiratory synchronization.

(2) Cardiorespiratory phase locking and frequency locking take place when respiratory oscillations become regular enough and have a particular frequency relation coupled with cardiac oscillations. We observed that the intermittence of respiratory oscillation varies with time but synchronization persists in some subjects, such as codes f1o06 and f1y05. This confirms correlations in the cardiorespiratory synchronization.



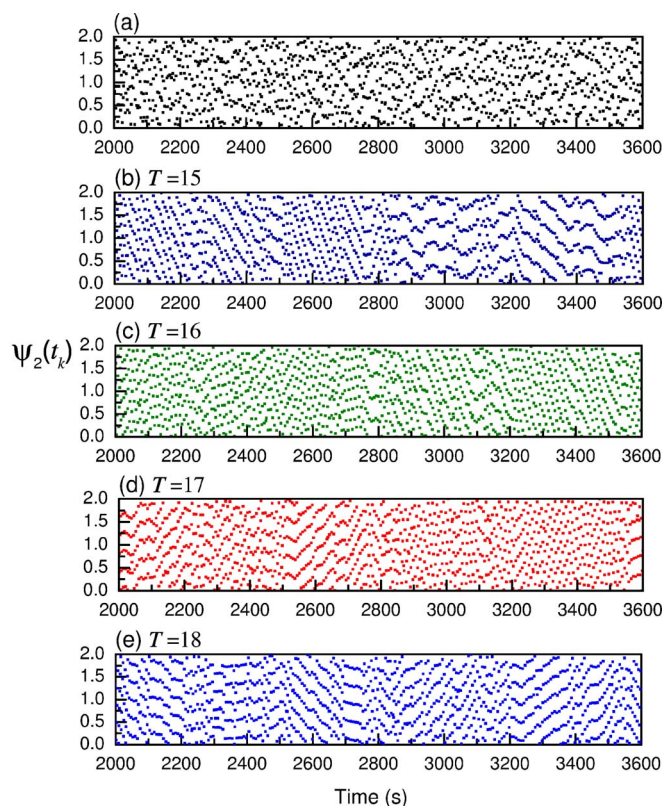


FIG. 8. (Color online) Cardiorespiratory synchronogram for data sets (a) (f1o09.res, f1o09.hrt) and  $[s(S_0=1000, T, t), f1o09.hrt]$ , with  $T=(b) 15, (c) 16, (d) 17, \text{ and } (e) 18$ .

(3) Overfiltered respiratory signals may be too regular, and in turn, appear to have stronger synchronization than they should have. Therefore, if the Fourier-based approach with narrow band filtration is used, some epochs of phase locking or frequency locking should be considered as originating from these effects.

## V. DISCUSSION

We have used the EMD method and CRS to study the synchronization between human heartbeat and respiration. The reason for using this method is that it is considered to be able to catch the primary structures of respiratory rhythms based on its adaptive features [38]. By imposing intermittency criteria based on physiological conditions revealed from empirical time series, this feature allows us to effectively keep the signal structures and avoid the introduction of artificial signals which easily appear in the Fourier-based filters with *a priori* bases that cannot process properly variable intermittencies in a nonlinear time series. Furthermore, the introduction of IMFs in the EMD provides a reasonable definition of the instantaneous phase. This advantage is considered to be helpful for drawing reliable conclusions on the studies of empirical data. From our results, we also found the existence of cardiorespiratory synchronization with several locking ratios occurring in several subjects as in Refs. [5,6], and there was one subject having phase locking lasting up to 800 s. However, significant relations between the occurrence

of synchronization and the sex and age of the subjects were not found in our results. At the current stage, even though cardiorespiratory synchronization has been observed in a number of studies, there is still no confident conclusion about its dependence on sex and age because few subjects were studied and most of the experiments were performed in different physiological stages. Although the tendency of cardiorespiratory synchronization to become weaker with increasing RSA was observed in earlier studies [5,6], the inferences about the strength of cardiorespiratory synchronization from the relation of the appearance of RSA and age may be misleading since ages usually do not reflect the same real physiological stage in different countries. Furthermore, the statistics of our results indicates most synchronization exhibits 3:1 (eight subjects), 4:1 (one subject), and 7:2 (four subjects) synchronization, which is consistent with the report of Ref. [12] that mature physiological subjects (adults) have larger probabilities of 3:1, 4:1, and 7:2 synchronization than 5:2 synchronization. Be aware that the subjects we studied in this paper are few; further investigations are required to draw global conclusions on these issues. In this context, our studies may be considered as constituting the statistics for further studies.

In this paper, we also discuss the origin of the cardiorespiratory synchronization from the viewpoint of signal characteristics: correlation and regularity. Regarding the results obtained by using the EMD method as a reference, we found that even though CRS can exhibit correlation between cardiac and respiratory signals, the strength of the synchronization (dominantly contributed by the regularity of respiratory signals) may not be precisely calculated. We then conclude that the existence of cardiorespiratory synchronization is true, but the strength (duration) of the synchronization could be dependent on the method used.

From a physiological viewpoint, it is difficult to precisely identify the mechanisms responsible for the observed nonlinear interactions. In particular, the human heart and respiratory systems are coupled by several mechanisms. Even though some early studies have suggested that cardiorespiratory synchronization is related to neural systems [5,6], the mechanical effects of respiratory motion may also induce frequency locking and phase locking. From our studies, we found that cardiac oscillations are more regular than respiratory oscillations, and cardiorespiratory synchronization occurs at the period when respiratory signals become regular enough. In other words, the regularity of respiratory signals contributes dominantly to the synchronization. Thus cardiorespiratory synchronization and RSA are two competing factors in the cardiorespiratory interactions. Our observations are indeed consistent with the results reported in Refs. [21,39]. Recently, Rosenblum and Pikovsky [39] proposed a technique for experimental detection of the directionality of weak coupling between two self-sustained oscillatory systems, based on the Fourier approximation of phase increments or instantaneous periods as a function of the phases, or on mutual predictability of the instantaneous phase. Paluš and Stefanovska [21] further proposed a directionality index to distinguish unidirectional from bidirectional coupling. Their studies demonstrated that the respiration is driving the cardiac system in a large part of the recording [21,39]. Such results are consistent with our observation.

Besides the limitations of experiments, our knowledge of the rhythm coordination of the subsystems in the body is still incomplete. As we have shown in this paper, using a simple (or, more complicated, a time-varying) cosine wave as respiratory signal and a time-varying ECG signal may produce a synchrogram similar to a real one. This makes modeling too easy to check its validity.

Our studies cannot point out the mechanism behind the synchronization phenomena, but can benefit investigations of the phenomena. Nevertheless, the improvements of respiration and heartbeat data processing indeed allow more reliable and precise analysis. In particular, regardless of the origin of the synchronization, an interesting question in clinical practice is whether rhythm coordination is a sign of good physical condition. The methods we used in this paper can contribute to signal analyses for clinical practice and academic studies.

Furthermore, the technique used in this paper can also be applied to the analysis of other time series, such as returns of

financial markets [40,41]. In the present paper, we consider only synchronization between two variables. Synchronization among many variables has been studied extensively in recent years [42]. It is of interest to extend the method of the present paper to analyze signals from many-body systems (e.g. signals of a set of neurons) and study their synchronization.

#### ACKNOWLEDGMENTS

This work was supported by Academia Sinica (Taiwan) under Grant No. AS-91-TP-A02, and the National Science Council of the Republic of China (Taiwan) under Grants No. NSC 93-2112-M-001-027 and No. NSC 94-2119-M-002-001. Part of this work was done while M.C.W. was visiting the Beth Israel Deaconess Medical Center at the Harvard Medical School (Boston, USA). He thanks Professor Ary L. Goldberger, Professor C.-K. Peng, and the Rey Laboratory for kind hospitality.

- 
- [1] A. C. Guyton, *Textbook of Medical Physiology*, 8th ed. (Saunders, Philadelphia, 1991).
- [2] L. Bernardi, F. Salvucci, R. Suardi, P. L. Solda, A. Calciati, S. Perlini, C. Falcone, and L. Ricciardi, *Cardiovasc. Res.* **24**, 969 (1990).
- [3] J. Almasi and O. H. Schmitt, *IEEE Trans. Biomed. Eng.* **21**, 264 (1974).
- [4] P. Tass, M. G. Rosenblum, J. Weule, J. Kurths, A. Pikovsky, J. Volkmann, A. Schnitzler, and H.-J. Freund, *Phys. Rev. Lett.* **81**, 3291 (1998).
- [5] C. Schäfer, M. G. Rosenblum, J. Kurths, and H.-H. Abel, *Nature (London)* **392**, 239 (1998).
- [6] C. Schäfer, M. G. Rosenblum, H.-H. Abel, and J. Kurths, *Phys. Rev. E* **60**, 857 (1999).
- [7] M. G. Rosenblum, J. Kurths, A. Pikovsky, C. Schäfer, P. Tass, and H.-H. Abel, *IEEE Eng. Med. Biol. Mag.* **17**, 46 (1998).
- [8] E. Toledo, S. Akselrod, I. Pinhas, and D. Aravot, *Med. Eng. Phys.* **24**, 45 (2002).
- [9] E. Toledo, M. G. Rosenblum, C. Schäfer, J. Kurths, and S. Akselrod, in *Proceedings of the International Symposium on Nonlinear Theory and its Applications* (Presses Polytechniques et Universitaires Romandes, Lausanne, 1998), Vol. 1, pp. 171–174.
- [10] E. Toledo, M. G. Rosenblum, J. Kurths, and S. Akselrod, *Comput. Cardiol.* **26**, 237 (1999).
- [11] M. B. Lotric and A. Stefanovska, *Physica A* **283**, 451 (2000).
- [12] R. Mrowka and A. Patzak, *Int. J. Bifurcation Chaos Appl. Sci. Eng.* **10**, 2479 (2000).
- [13] A. Stefanovska, H. Haken, P. V. E. McClintock, M. Hozic, F. Bajrovic, and S. Ribaric, *Phys. Rev. Lett.* **85**, 4831 (2000).
- [14] K. Kotani, K. Takamasu, Y. Ashkenazy, H. E. Stanley, and Y. Yamamoto, *Phys. Rev. E* **65**, 051923 (2002).
- [15] M. G. Rosenblum, A. S. Pikovsky, and J. Kurths, *Phys. Rev. Lett.* **76**, 1804 (1996).
- [16] R. Quian Quiroga, J. Arnhold, and P. Grassberger, *Phys. Rev. E* **61**, 5142 (2000).
- [17] R. Quian Quiroga, A. Kraskov, T. Kreuz, and P. P. Grassberger, *Phys. Rev. E* **65**, 041903 (2002).
- [18] M. G. Rosenblum, A. S. Pikovsky, and J. Kurths, *Fluct. Noise Lett.* **4**, L53 (2004).
- [19] M. G. Rosenblum and A. S. Pikovsky, *Phys. Rev. Lett.* **92**, 114102 (2004).
- [20] T. Schreiber, *Phys. Rev. Lett.* **85**, 461 (2000).
- [21] M. Paluš and A. Stefanovska, *Phys. Rev. E* **67**, 055201(R) (2003).
- [22] J. Jamsek, A. Stefanovska, and P. V. E. McClintock, *Phys. Med. Biol.* **49**, 4407 (2004).
- [23] M. Richter, T. Schreiber, and D. T. Kaplan, *IEEE Eng. Med. Biol. Mag.* **45**, 133 (1998).
- [24] R. Hegger, H. Kantz, and T. Schreiber, *Chaos* **9**, 413 (1999).
- [25] H. Kantz and T. Schreiber, *IEE Proc.: Sci., Meas. Technol.* **145**, 279 (1998).
- [26] D. Gabor, *J. Inst. Electr. Eng., Part 1* **93**, 429 (1946).
- [27] S. Blanco, R. Q. Quiroga, O. A. Rosso, and S. Kochen, *Phys. Rev. E* **51**, 2624 (1995).
- [28] S. Blanco, C. E. D'Attellis, S. I. Isaacson, O. A. Rosso, and R. O. Sirne, *Phys. Rev. E* **54**, 6661 (1996).
- [29] S. Blanco, A. Figliola, R. Quian Quiroga, O. A. Rosso, and E. Serrano, *Phys. Rev. E* **57**, 932 (1998).
- [30] K. Ohashi, L. A. Nunes Amaral, B. H. Natelson, and Y. Yamamoto, *Phys. Rev. E* **68**, 065204(R) (2003).
- [31] K. Karhunen, *Ann. Acad. Sci. Fenn., Ser. A* **37**, 3 (1946).
- [32] M. M. Loève, *Probability Theory* (Van Nostrand, Princeton, NJ, 1955).
- [33] N. E. Huang, Z. Shen, S. R. Long, M. C. Wu, H. H. Shih, Q. Zheng, N.-C. Yen, C.-C. Tung, and H. H. Liu, *Proc. R. Soc. London, Ser. A* **454**, 903 (1998).
- [34] Besides the Hilbert spectral analysis, one can also use other methods to process the data obtained from EMD; see, e.g., Refs. [16,17].
- [35] M. Chavez, C. Adam, V. Navarro, S. Boccaletti, and J. Martinerie, *Chaos* **15**, 023904 (2005).

- [36] N. E. Huang, M. C. Wu, S. R. Long, S. S. P. Shen, W. Qu, P. Gloersen, and K. L. Fan, *Proc. R. Soc. London, Ser. A* **459**, 2317 (2003).
- [37] N. Iyengar, C.-K. Peng, R. Morin, A. L. Goldberger, and L. A. Lipsitz, *Am. J. Physiol.* **271**, 1078 (1996). Data sets are available from <http://physionet.org/physiobank/database/fantasia/>
- [38] The power and confidence limit of the EMD method for various empirical time series have been justified and discussed thoroughly in Refs. [33,36].
- [39] M. G. Rosenblum and A. S. Pikovsky, *Phys. Rev. E* **64**, 045202(R) (2001).
- [40] M.-C. Wu, M.-C. Huang, H.-C. Yu, and T. C. Chiang, *Phys. Rev. E* **73**, 016118 (2006).
- [41] M.-C. Wu (unpublished).
- [42] P. M. Gade and C. -H. Hu, *Phys. Rev. E* **60**, 4966 (1999); *ibid.* **62**, 6409 (2000); *ibid.* **73**, 036212 (2006); S. Jalan, R. E. Amritkar, and C. -K. Hu, *ibid.*, **72**, 016211 (2005); R. E. Amritkar, S. Jalan and C. -K. Hu, *ibid.*, **72**, 016212 (2005); R. E. Amritkar and C. -K. Hu, *Chaos* **16**, 015117 (2006).